Pergamon

0301-9322(93)E0028-4

Int. J. Multiphase Flow Vol. 20, No. 3, pp. 613–629, 1994
Copyright © 1994 Elsevier Science Ltd
Printed in Great Britain. All rights reserved
0301-9322/94 $7.00 + 0.00

THE DRAINAGE AND RUPTURE OF PARTIALLY-MOBILE FILMS BETWEEN COLLIDING DROPS AT CONSTANT APPROACH VELOCITY

S. ABID[1] and A. K. CHESTERS[2]†

[1]Institut de Mécanique des Fluides de Toulouse, Avenue du Professeur Camille Soula, 31400 Toulouse, France

[2]Laboratory of Fluid Dynamics and Heat Transfer, Eindhoven University of Technology, P.O. Box 513, Eindhoven, The Netherlands

(Received 2 April 1993; in revised form 22 November 1993)

Abstract—A numerical study is presented of the drainage and rupture of the liquid film between two drops whose centres approach each other at constant velocity. The considerations are restricted to the partially-mobile case (in which the drop viscosity is rate-determining) and to small approach velocities. The latter restriction permits a transformation of the governing equations to a single universal form, which is solved with the help of boundary integral theory. As in the constant force case, the numerical results show the formation of a dimple but the final drainage behaviour differs considerably. Finally, the influence of van der Waals forces is investigated and the results are shown to correspond well with a simple model proposed earlier for the effective critical film-rupture thickness.

Key Words: coalescence, drops, liquid film, drainage, rupture, van der Waals force, boundary integral technique

1. INTRODUCTION

Drop coalescence processes are an essential feature of a great number of industrial and environmental liquid–liquid systems. A review of the current understanding, henceforth referred to as paper I, has recently been provided by Chesters (1991). The complex physico-chemical hydrodynamics of coalescence processes induced by drop collisions can be split conceptually into three elements:

- The external flow field which determines the frequency, interaction force and duration of collisions.
- The internal flow field involved in drainage of the residual film between the drops, for which the initial and boundary conditions are provided by the external flow.
- The destabilization of very thin films by colloidal forces, leading to rupture.

Even in the simplest case of pure liquids, these elements have yet to be modelled adequately. One of the major unanswered questions is the dependence of the film drainage process on the boundary conditions provided by the collision, which will not, in general, correspond to the case examined to date in the literature, of constant interaction force.

In this paper, the problem tackled concerns the drainage and rupture of a partially-mobile film of continuous phase between two drops undergoing a gentle, constant-velocity collision along the line of their centres. The term partial mobility is used here, as in paper I, to indicate that drainage is controlled by the motion of the film surface (the Poiseuille contribution to the film flow being negligible in comparison), which in turn is limited by the shear stress exerted by the drop phase. The term gentle is used to indicate that only a small portion of each drop surface is deformed significantly. This enables a major simplification of the governing equations (section 2.1), which become the same for unequal drops (radii R_1 and R_2) as for equal drops of radius R_{eq}, where

$$R_{eq}^{-1} = \frac{R_1^{-1} + R_2^{-1}}{2}. \qquad [1]$$

†To whom correspondence should be addressed.

This regime has been examined by Yiantsios & Davis (1990), who termed it that of full mobility, in the viscous, constant-interaction-force limit, in the context of a small drop rising to a free interface. Making use of the equivalent-radius construct ($R_2 = \infty$, $R_{eq} = 2R$), together with a suitable transformation of the governing equations, their numerical solutions can be shown to apply to all constant-force drainage processes (paper I). In a subsequent paper, Yiantsios & Davis (1991) extend the considerations on the one hand to the gravity-driven approach of coaxially-rising drops and on the other to include the effect of destabilizing van der Waals forces (immobile-interface case only).

While film drainage at a free interface under the influence of gravitational forces provides an important example of a constant-force collision, it is probably the only one. In other cases, collisions are flow-driven and the interaction force increases as the drops approach, reaching a maximum in the absence of coalescence and falling off as the drops separate. The drops may be free, as in agitated dispersions, or one or both may be attached, as in the respective cases of filter coalescers and injection through porous surfaces. Depending on the collision Reynolds number, the interaction force may be due primarily to viscous or inertial forces. The latter case is characterized initially by constant approach velocity, this velocity diminishing only when deformation becomes sufficient to convert a substantial proportion of the kinetic energy of the collision into interfacial energy (paper I; Chesters & Hofman 1982). The constant-velocity case is thus of some practical relevance, in addition to its interest as a well-defined alternative boundary condition for film drainage.

In section 2, the governing equations and initial and boundary conditions are derived for the constant-velocity case in the absence of van der Waals forces. These are then cast into dimensionless form, after which the only dimensionless group (a Capillary number) is eliminated by means of a transformation of variables, leading, as in the constant-force case, to a universal set of equations describing all such processes. The numerical solution of these equations is presented in section 3 and the similarities with and differences from the constant-force case examined. Both solutions are furthermore compared with the plane-film model developed by Chesters (1988). In section 4, van der Waals forces are included and their effect on the solutions compared with that predicted by approximate considerations (paper I). Finally, in section 5, the regime of validity of various approximations underlying the solutions is examined.

2. GOVERNING EQUATIONS IN THE ABSENCE OF VAN DER WAALS FORCES

2.1. The Equations in Dimensional Form

2.1.1. Underlying approximations

The film-draining equations are simplified by a number of restrictions/approximations which were also applied in the analysis of Yiantsios & Davis (1990):

(i) The restriction to gentle (axisymmetrical) collisions, involving small deformed portions of the drops, implies small film slopes:

$$\left|\frac{\partial(h_i)}{\partial r}\right| \ll 1 \qquad [2]$$

(h_i is the z-coordinate of the interface, $i = 1, 2$; r is the radial coordinate—see figure 1).

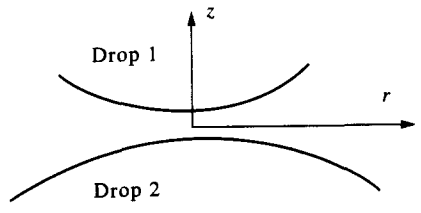

Figure 1. Choice of coordinates for the description of film drainage.

(ii) Considerations are limited to the viscous regime, in which the inertial forces are negligible both in the film and in the adjacent dispersed-phase flow (though not necessarily in the overall flow involved in the drop collision).
(iii) The restriction to partial mobility, as defined above, permits the film flow to be approximated as plug flow and the influence of viscous normal stresses in the film to be neglected, the shear stress exerted by the dispersed phase being rate-controlling.
(iv) The latter statement implicitly neglects the effect on film drainage of any variation in pressure or in the viscous normal stress in the dispersed phase.
(v) Finally, the influence is neglected of body forces due to gravity or to acceleration of the reference frame, whose origin is chosen at the film centre (figure 1).

The regime of validity of (i)–(v) is considered in section 5.

2.1.2. Flow in the film

Making use of [2], the continuity and Navier–Stokes equations, applied in an integrated form to an element of film, become

$$\frac{\partial h}{\partial t} = -\frac{1}{r}\frac{\partial (rhu)}{\partial r} \qquad [3]$$

and

$$\tau = -\frac{h}{2}\frac{\partial p}{\partial r} \qquad [4]$$

(h is the film thickness, $h_1 - h_2$; t is time; u is the interface velocity or, equivalently, the radial component of the film velocity, in view of approximation (iii); τ is the shear stress exerted on the interface in the r-direction by the film phase; p is the pressure in the film). Note that in view of the quasi-parallel character of the film flow, p is constant across the film.

2.1.3. Flow in the drops

For the quasi-steady creeping flow in the drops, the continuity and Navier–Stokes equations are:

$$\nabla \cdot \mathbf{v} = 0 \qquad [5]$$

and

$$-\nabla p_d + \mu_d \nabla^2 \mathbf{v} = 0 \qquad [6]$$

(the subscript d denotes the dispersed phase; μ is the dynamic viscosity; $\mathbf{v}$ is the dispersed-phase velocity).

2.1.4. Interface conditions

The conditions to be satisfied at the interfaces are

$$u = v_r \qquad [7]$$

$$\tau + \tau_d = 0 \qquad [8]$$

and

$$p_d - p = \sigma(R_a^{-1} + R_b^{-1}) \qquad [9]$$

(σ is the interfacial tension; R_a and R_b are the principal radii of curvature of the interface). Equation [7] expresses continuity of velocity. Equation [8] expresses the requirement that the net tangential stress exerted on the interface be zero; note that τ_d is the same for each interface, since the film drainage induces the same flow in each drop, the drop interface being effectively a plane on the scale of the drop flow, in view of [2]. Equation [9] is the Laplace condition on the jump in the normal stress, neglecting the contibution of the viscous normal stresses [approximations (iii) and (iv)]. Making use of [2] with the relevant expressions for R_a and R_b, together with the fact that outside the deformed region $p \to 0$ so that $p_d = 2\sigma/R_i$, [9] yields an equation for each interface:

$$p = \frac{2\sigma}{R_1} - \sigma\left(\frac{\partial^2 h_1}{\partial r^2} + \frac{1}{r}\frac{\partial h_1}{\partial r}\right) \quad [10a]$$

and

$$p = \frac{2\sigma}{R_2} + \sigma\left(\frac{\partial^2 h_2}{\partial r^2} + \frac{1}{r}\frac{\partial h_2}{\partial r}\right) \quad [10b]$$

Subtraction of [10a,b], yields an equation for the film centre coordinate, z_c:

$$\frac{\partial^2 z_c}{\partial r^2} + \frac{1}{r}\frac{\partial z_c}{\partial r} = \frac{2}{R_c}, \quad [11a]$$

where

$$z_c = \frac{1}{2}(h_1 + h_2), \quad \frac{1}{R_c} = \frac{1}{2}\left(\frac{1}{R_1} - \frac{1}{R_2}\right). \quad [11b,c]$$

Integrating [11a] twice yields

$$z_c = \frac{r^2}{2R_c}, \quad [12]$$

indicating that the centre surface is spherical (to the first order in the interface slope), with radius of curvature R_c. Addition of [10a,b] yields

$$p = \frac{2\sigma}{R_{eq}} - \frac{\sigma}{2}\left(\frac{\partial^2 h}{\partial r^2} + \frac{1}{r}\frac{\partial h}{\partial r}\right), \quad [13]$$

indicating that the equations for unequal drops are the same as those for equal drops of radius R_{eq}.

2.1.5. Initial and boundary conditions

The chosen initial condition is of undeformed drops. From [9], p is then zero and [13] may be integrated twice to yield

$$h = h_0 + \frac{r^2}{R_{eq}}. \quad [14]$$

This should provide a good approximation to the situation of approach from infinity, provided the thickness at the film centre h_0 is chosen sufficiently large. The outer boundary conditions are

$$p = 0, \quad \frac{\partial h}{\partial t} = -V, \quad [15a,b]$$

at sufficiently large r-values, corresponding to undeformed interfaces (V is the drop approach velocity).

2.2. Transformed Equations

The first step in eliminating as many as possible of the system parameters μ_d, σ, R_{eq} and V is to render the variables in the governing equations dimensionless with the help of R_{eq}, V and μ_d:

$$r' = \frac{r}{R_{eq}}; \quad h' = \frac{h}{R_{eq}}; \quad t' = \frac{tV}{R_{eq}}; \quad \tau' = \frac{\tau R_{eq}}{\mu_d V}; \quad p' = \frac{pR_{eq}}{\mu_d V}; \quad \mathbf{u}' = \frac{\mathbf{u}}{V}; \quad \mathbf{v}' = \frac{\mathbf{v}}{V}.$$

The new equations contain only one system parameter, the Capillary number, Ca ($=\mu_d V/\sigma$). This too is eliminated by a suitable transformation in powers of Ca:

$$r^* = \frac{r'}{Ca^{1/3}}; \quad h^* = \frac{h'}{Ca^{2/3}}; \quad t^* = \frac{t'}{Ca^{2/3}}; \quad \tau^* = \tau' Ca^{2/3}; \quad p^* = p' Ca; \quad \mathbf{u}^* = \mathbf{u}' Ca^{1/3}; \quad \mathbf{v}^* = \mathbf{v}' Ca^{1/3}.$$

The transformed governing equations now become:

$$\frac{\partial h^*}{\partial t^*} = -\frac{1}{r^*}\frac{\partial (h^* u^* r^*)}{\partial r^*}, \quad [3^*]$$

$$\tau^* = -\frac{h^*}{2}\frac{\partial p^*}{\partial r^*}, \qquad [4^*]$$

$$\nabla^* \cdot \mathbf{v}^* = 0, \qquad [5^*]$$

$$-\nabla^* p_d^* + \nabla^{*2}\mathbf{v}^* = 0, \qquad [6^*]$$

$$u^* = v_r^*, \qquad [7^*]$$

$$\tau^* + \tau_d^* = 0, \qquad [8^*]$$

$$p^* = 2 - \frac{1}{2}\left(\frac{\partial^2 h^*}{\partial r^{*2}} + \frac{1}{r^*}\frac{\partial h^*}{\partial r^*}\right), \qquad [13^*]$$

$$h^* = h_0^* + r^{*2}, \quad \text{at } t^* = 0 \qquad [14^*]$$

and

$$p^* = 0, \quad \frac{\partial h^*}{\partial t^*} = -1, \quad \text{at } r^* \to \infty. \qquad [15a^*,b^*]$$

3. NUMERICAL SOLUTION

3.1. *Method of Solution*

The relation between τ^* and u^* implied by the creeping-flow equations [5*] and [6*] is provided by the boundary integral theory, applied to the flow in the half space concerned (Davis *et al.* 1989):

$$u^*(r^*) = \int_0^\infty \phi(r^*, r')\tau^*(r')\,dr', \qquad [16a^*]$$

where

$$\phi(r^*, r') = \frac{r'}{4\pi}\int_0^{2\pi} \frac{\cos\theta\,d\theta}{(r^{*2} + r'^2 - 2r^*r'\cos\theta)^{1/2}} \qquad [16b^*]$$

is an elliptic type Green's function kernel.

The system of equations [3*]–[15b*] can be solved numerically for the unknowns: thickness, pressure, interfacial stress and velocity. Given the film shape [14*] at $t^* = 0$, p^* follows from [13*], τ^* from [4*], u^* then follows from [16*] and $\partial h^*/\partial t^*$ from [3*]. The new film shape can now be computed at a time Δt^* later and the whole process repeated.

In the calculation of u^*, the interface was approximated as flat and unbounded. In practice, we must truncate the domain of the interface at some large but finite distance, r^*_{bound}, from the axis of symmetry. A non-uniform discretization of the interface was employed: a constant, relatively small Δr^* near the axis of symmetry which is a region of high property gradients, and far from this region, progressively larger Δr^*. To calculate the integral, a trapezoidal rule is used. Fourth-order central-difference approximations were used for the spatial derivatives ($\partial h^*/\partial r^*$) and ($\partial^2 h^*/\partial r^{*2}$); while the ($\partial^3 h^*/\partial r^{*3}$) term was approximated by a second-order central difference.

The continuity equation [3*] is solved by using a Lax–Wendroff finite-difference scheme of second-order accuracy. The values of h_0^* and r^*_{bound} proved of little influence, provided they were chosen sufficiently large.

3.2. *Results and Discussion*

Figure 2 shows the variation of the film thickness h^* with r^* and t^*. The results indicate that the drops flatten and then develop a dimple. The development of a dimple is also found in the constant-force case (Yiantsios & Davis 1990).

The variation of the pressure in the film p^* is presented in figure 3. The transformed pressure at the centre of the film increases as the drops move toward each other until it reaches a value of 2, indicating the onset of complete flattening (the dimensionless curvature terms $\partial^2 h^*/\partial r^{*2}$ and $(1/r^*)\partial h^*/\partial r^*$, which are equal at the film centre, then being zero: [13*]). The size of the flattened

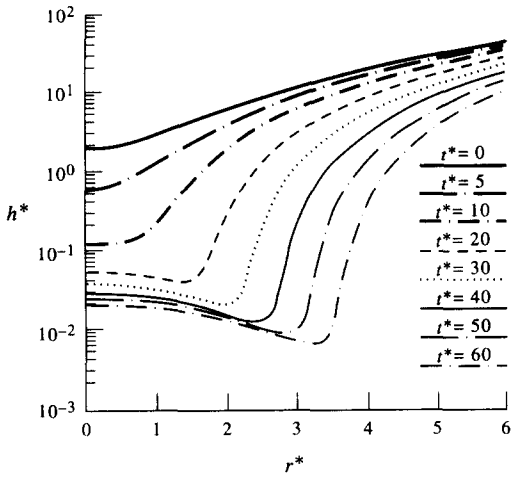

Figure 2. Variation of the film thickness during the drainage process; $h_0^* = 2$, $r_{bound}^* = 20$.

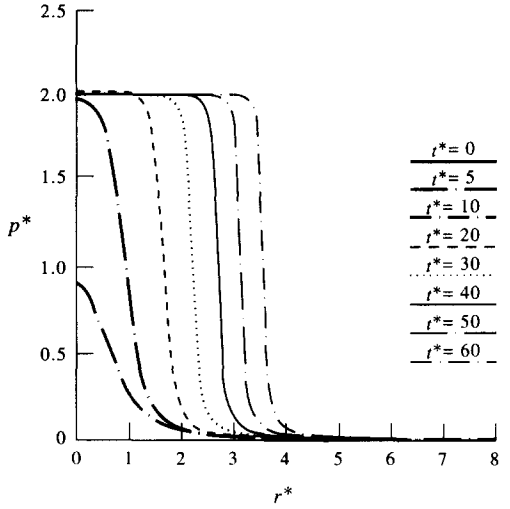

Figure 3. Variation of the pressure during the drainage process.

region increases with time, as it must since the drop centres continue to approach each other. A measure, a, of the radius of the flattened region may be defined by

$$F = \int_0^{r^* \text{large } r} 2\pi r p \, dr = \pi a^2 \left(\frac{2\sigma}{R_{eq}}\right) \qquad [17]$$

(F is the drop interaction force). Figure 4 shows the increase with t^* of $(a^*)^2$, which is a measure of the interaction force. The time dependence of $(a^*)^2$ is similar to that predicted by the simple deformation model of figure 5 (see the appendix),

$$(a^*)^2 = \tfrac{1}{2}(t^* - h_0^*), \qquad [18]$$

though the actual values of a^* are appreciably smaller. As would be expected, the transformed radius r_{min}^*, at which the minimum film thickness is attained, is proportional to a^* once flattening has occurred (figure 6).

The variations of the transformed film velocity, u^*, and the shear stress, τ^*, are presented in figures 7 and 8. After the formation of the dimple, the u^* and τ^* maxima are situated close to r_{min}^*. The maximum of the film velocity decreases with time, in contrast with the fully-mobile,

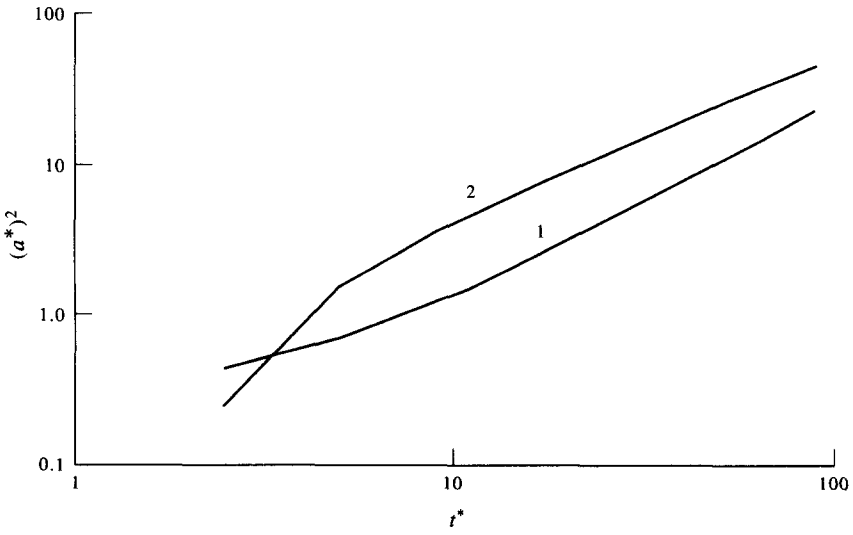

Figure 4. $(a^*)^2$ as a function of time: **1**, $(a^*)^2 = \int_0^{r^* \text{large } r^*} r^* p^* \, dr^*$; **2**, $(a^*)^2 = \frac{1}{2}(t^* - h_0^*)$.

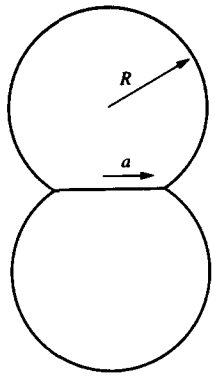

Figure 5. Idealized deformation during the collision of two equal drops.

inertia-dominated case (Chesters & Hofman 1982) where the presence of the dimple leads to increasingly large values of velocity.

After the dimple has established itself, film thinning develops an asymptotic character (figure 9), the thickness at the film center, h^*_{cen}, and the minimum thickness, h^*_{min}, obtained from the numerical results, decaying approximately as

$$h^*_{cen} = 0.58(t^*)^{-0.8}, \quad h^*_{min} = 4.8(t^*)^{-1.6}, \qquad [19,20]$$

in contrast with the constant-force case where the corresponding exponents are $(-1/3)$ and $(-2/3)$.

3.3. Comparison with the Constant-force and Plane-film Cases

The governing equations in the constant-force case can be cast into universal form (paper I) if expressed in terms of the transformed variables:

$$h^+ = \frac{h}{\dfrac{3a^2}{2R_{eq}}}; \quad r^+ = \frac{r}{\dfrac{\sqrt{3}a}{2}}; \quad t^+ = \frac{t}{\dfrac{\mu_d R_{eq}^2}{\sqrt{12}\sigma a}}. \qquad [21a\text{–}c]$$

The $^+$ and * variables are readily seen to be related as:

$$\frac{h^+}{h^*} = \frac{2}{3(a^*)^2}; \quad \frac{r^+}{r^*} = \frac{2}{\sqrt{3}a^*}; \quad \frac{t^+}{t^*} = \sqrt{12}a^*. \qquad [22a\text{–}c]$$

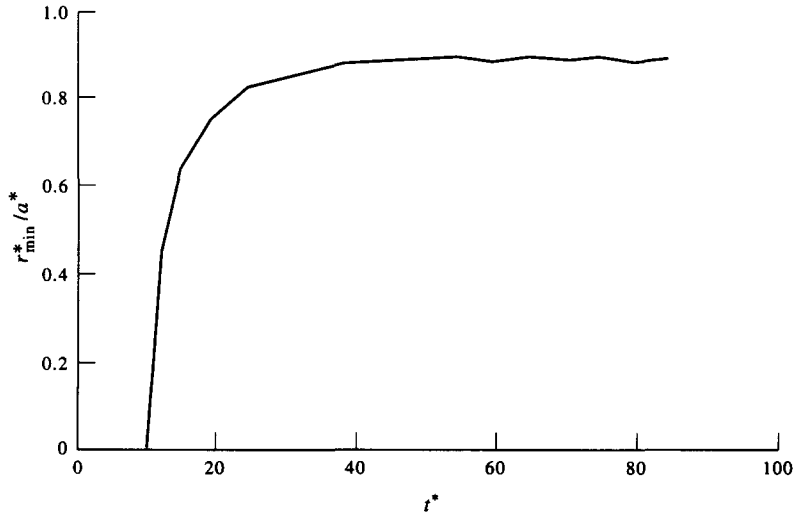

Figure 6. (r^*_{min}/a^*) as a function of time.

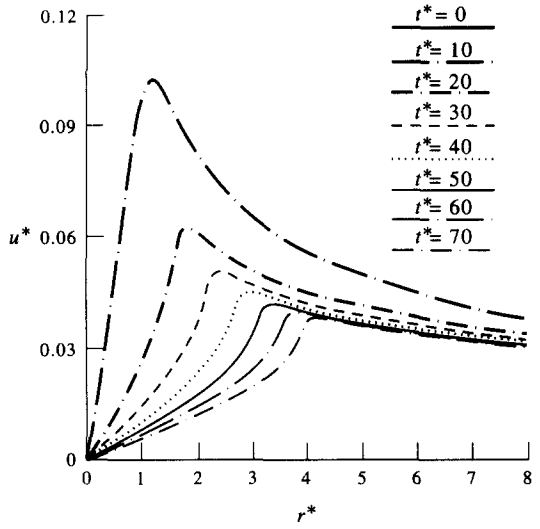

Figure 7. Variation of the film velocity during the drainage process.

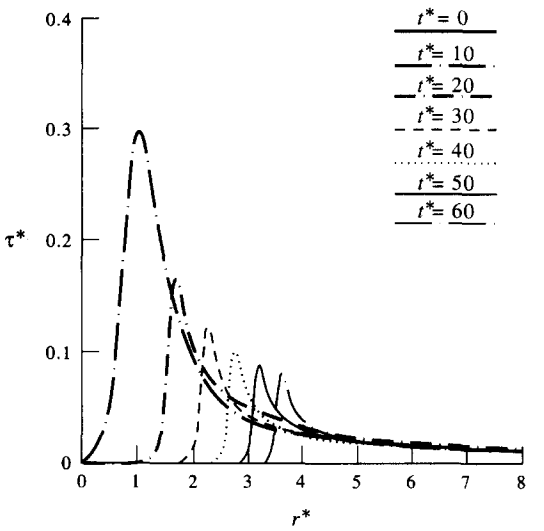

Figure 8. Variation of the shear stress during the drainage process.

Figure 10 displays the results of Yiantsios & Davis for this case, expressed in terms of $^+$ variables, together with those of a plane-film model (Chesters 1988; paper I) which predicts that

$$-\frac{1}{(h^+)^2}\frac{\mathrm{d}h^+}{\mathrm{d}t^+} = \mathrm{k}, \qquad [23]$$

where the constant k is of order unity. Evidently [23], taking k = 0.66, provides a good description just after flattening sets in ($h^+ \approx 10^{-1}$), becoming poorer as the dimple develops.

Applied to the constant-velocity case and expressed in terms of * variables, the plane-film drainage expression becomes

$$-\frac{a^*}{(h^*)^2}\frac{\mathrm{d}h^*}{\mathrm{d}t^*} = \left(\frac{4}{\sqrt{3}}\right)\mathrm{k} = 1.52. \qquad [24]$$

Table 1 presents the value of $(-a^*/(h^*_{\min})^2)\,\mathrm{d}h^*_{\min}/\mathrm{d}t^*$ in this case, following flattening at $h^* \approx 10^{-1}$. While the initial drainage rate corresponds reasonably well with [24], it subsequently becomes much

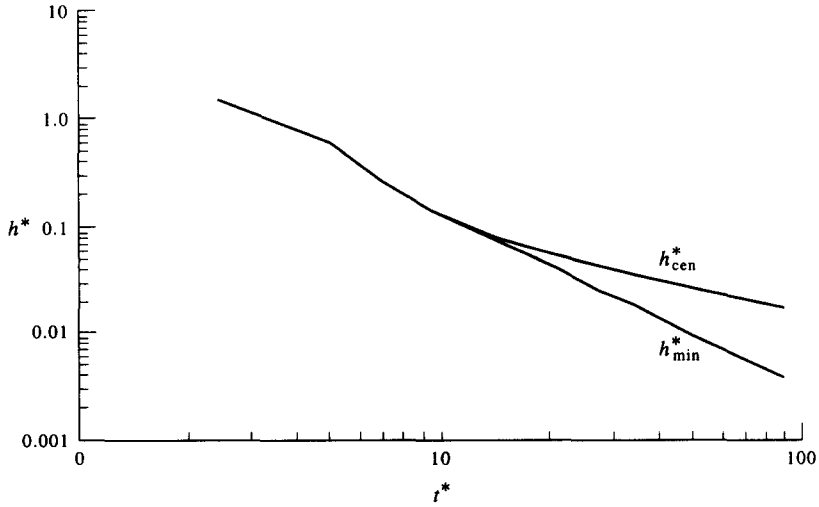

Figure 9. $h^*_{\min}$ and h^*_{cen} as functions of time.

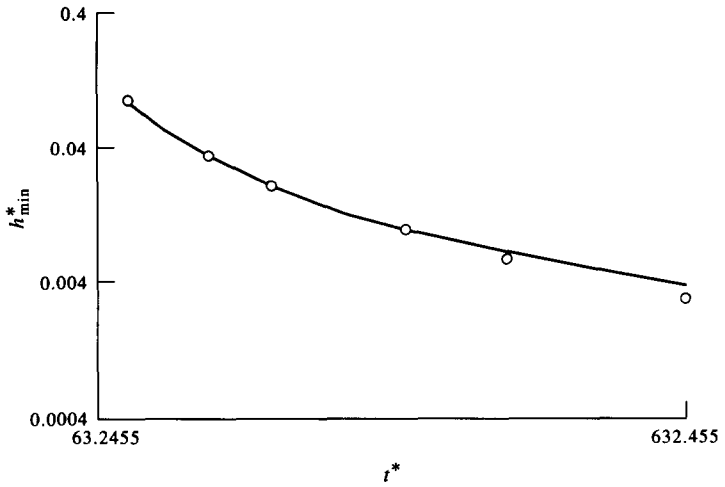

Figure 10. Comparison of the constant-force case [—, Yiantsios & Davis (1990)] and the plane-film model (○, [23] with k = 0.66).

larger, in contrast with the constant-force case where the plane-film approximation remains reasonable. Physically, this might be interpreted as indicating that the thickness of the "new film" added during expansion of the flattened region is smaller than that of the old.

A further difference between the constant-force and constant-velocity behaviour is the film thickness at which flattening sets in, which is an order of magnitude smaller in the latter case ($h^+ \approx 10^{-2}$, compared with 10^{-1}). Qualitatively this can be explained by the fact that constant-velocity conditions imply increasing interaction force (figure 4) so that, for a given h^+, the driving force for deformation in the preceding stages of drainage is less.

The major difference between the two cases emphasizes the importance of incorporating realistic boundary conditions when simulating the coalescence of colliding drops, neither the interaction force nor the velocity, in general, being constant.

4. FILM RUPTURE: THE INFLUENCE OF VAN DER WAALS FORCES

4.1. Governing Equations

Equation [20] implies that coalescence requires an infinite time unless one or more of the classical approximations underlying the governing equations breaks down. Amongst these assumptions are the continuum approximation and the representation of the effect of long-range intermolecular forces by an interfacial tension confined to a mathematically thin layer at the phase boundary. While the continuum approximation must fail when the film thickness becomes of the order of molecular dimensions, the second approximation fails still earlier, the film tension becoming a decreasing function of the film thickness once film thicknesses become of the order of the long-range intermolecular interaction forces. For pure systems, the non-retarded expressions are the relevant ones for the small film thicknesses at which these forces become important [see, for example, Hiemenz (1986)].

Table 1. The value of $-[a^*/(h^*_{min})^2]\, dh^*_{min}/dt^*$ in the constant-velocity case during the thinning process

t^*	h^*	$-[a^*/(h^*_{min})^2]\, dh^*_{min}/dt^*$
10	0.12849	1.53
20	0.0418	3.54
40	0.031	8.67
50	0.00908	11.26
70	0.00533	16.53
90	0.00363	20.74

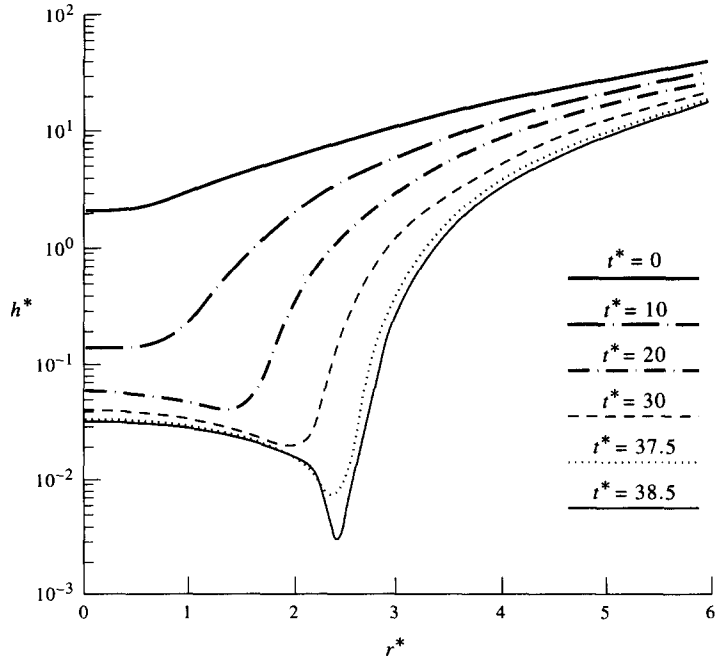

Figure 11. Variation of the film thickness when van der Waals forces are acting ($A^* = 10^{-5}$).

The van der Waals forces contribute an extra force, F_w, per unit volume of the film acting in the r-direction, given by (see, for example, paper I):

$$F_w = \frac{A}{2\pi h^4}\frac{\partial h}{\partial r}, \qquad [25]$$

where A denotes the Hamaker constant ($A \sim 10^{-20}$ J typically). The force balance [4] is then replaced by

$$-\frac{\partial p}{\partial r} + \frac{A}{2\pi h^4}\frac{\partial h}{\partial r} = \frac{2}{h}\tau, \qquad [26]$$

which in terms of transformed variables become

$$\tau^* = -\frac{h^*}{2}\frac{\partial p^*}{\partial r^*} + \frac{A^*}{h^{*3}}\frac{\partial h^*}{\partial r^*}, \qquad [27]$$

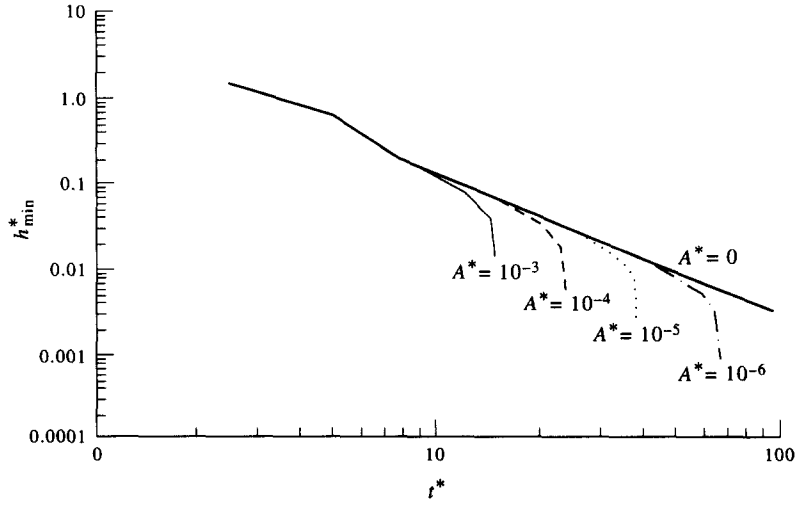

Figure 12. Minimum film thickness vs time for a range of A*-values.

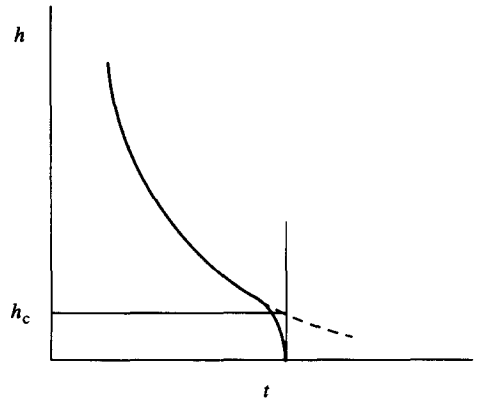

Figure 13. Influence of van der Waals forces on film drainage: ——, actual drainage behaviour; – – –, behaviour in the absence of van der Waals forces.

where

$$A^* = \frac{1}{4\pi} \frac{A}{\sigma R_{eq}^2 Ca^2}. \qquad [28]$$

Taking the same h_0^* and r_{bound}^* as the preceding case, the new set of equations is solved by the same method for various values of A*.

4.2. *Results*

In section 5, it is shown that the small-slope approximation requires that $Ca^{1/3} \ll 1$. Taking typical values of A and σ as 10^{-20} J and $2.5 \cdot 10^{-2}$ N/m, respectively, the A*-values of interest are seen to range from as little as 10^{-8} when $R_{eq} = 1$ mm and $Ca = 10^{-3}$ to 1 or more for small drops with very small Ca-values.

Figure 11 depicts the drainage process in the presence of van der Waals forces when $A^* = 10^{-5}$. van der Waals forces first become significant where the film is thinnest, thinning is accelerated locally and rupture quickly follows. Figure 12 shows the effect of A* on this process and on the rupture time, t_c^*. For the largest value of A*, 10^{-3}, van der Waals forces become important around the onset of flattening.

An effective critical film-rupture thickness, h_c^*, may be defined as the value of h_{min}^* which would be attained in the absence of van der Waals forces after a time t_c^* (figure 13). In paper I, it was suggested that h_c should be given by

$$h_c \approx \left(\frac{AR_{eq}}{8\pi\sigma}\right)^{1/3}. \qquad [29a]$$

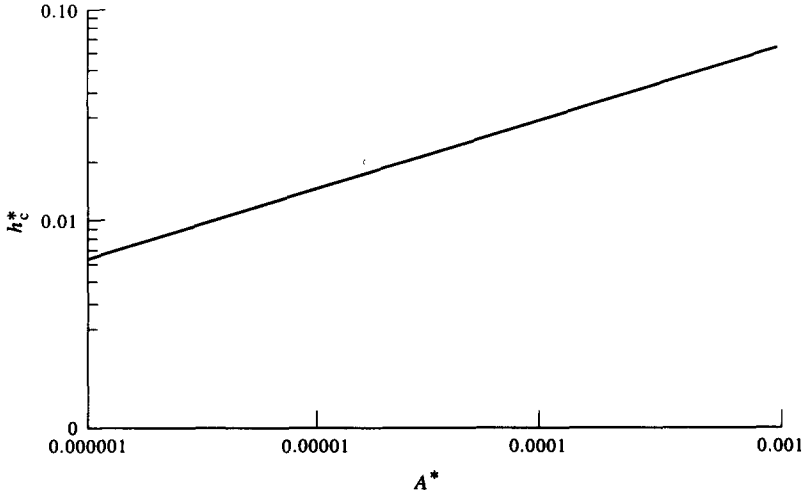

Figure 14. Critical film-rupture thickness, h_c^*, as a function of A*.

In transformed variables, [29a] becomes

$$h_c^* \approx \left(\frac{A^*}{2}\right)^{1/3}. \qquad [29b]$$

Figure 14 indicates that [29a,b] does indeed provide a good approximation, the best-fit straight line on a log–log plot being given by

$$h_c^* \approx 0.69(A^*)^{0.3377}. \qquad [30]$$

5. THE REGIME OF VALIDITY OF THE SOLUTION

Both the present results and those of Yiantsios & Davis (1990) for the constant-force case are based on the approximations listed in section 2.1. Each of these has its regime of applicability, whose boundary typically corresponds to a transition to another drainage regime in which an alternative approximation is better. The approximation of plug flow, for example, is justified provided the contribution to film drainage of the parabolic part of the film-velocity profile is negligible in comparison with the interface velocity. For sufficiently large μ_d/μ-values this will no longer be the case and a transition will take place to the immobile-interface regime, in which drainage is dominated by the parabolic contribution, the interface velocity being negligible.

In the context of the modelling of liquid–liquid dispersions, the primary question is the location in parameter space of the limiting surface dividing coalescing from non-coalescing collisions. The validity of the approximations need therefore only be considered under these limiting conditions, for which the drop interaction time, t_i, is equal to the required time for drainage to rupture, t_c. Since, furthermore, t_c is determined primarily by the last stage of drainage, the considerations may be restricted to the case when $h \sim h_c$. Even then the range of possible situations is immense, since t_i depends on the flow type, the drop size ratio and the incidence of the colliding particles. Here we consider only the simplest case of equal-drop collisions in viscous simple shear, making use of the approximate drainage and rupture relations [24] and [29].

5.1. Limiting Conditions for the Coalescence of Equal Drops in Viscous Simple Shear

From paper I it follows that the limiting conditions for which $t_i = t_c$ correspond to

$$\Omega^{3/2} \approx \frac{\mu}{\mu_d}\left(\frac{A}{8\pi\sigma R^2}\right)^{1/3}, \qquad [31]$$

where Ω denotes the dimensionless shear rate:

$$\Omega = \frac{\mu\dot{\gamma}R}{\sigma} \qquad [32]$$

($\dot{\gamma}$ is the shear rate). It was also shown that the film radius a is related to Ω by

$$\frac{a}{R} \approx (3\Omega)^{1/2}, \qquad [33]$$

so that [31] can alternatively be expressed as

$$\frac{a}{R} \approx \sqrt{3}\left(\frac{\mu}{\mu_d}\right)^{1/3}\left(\frac{A}{8\pi\sigma R^2}\right)^{1/9}. \qquad [34]$$

5.2. The Approximation of Plug Flow

The mean velocity, u_p, associated with the plane Poiseuille component of the film flow is given by

$$u_p = -\frac{h^2}{12\mu}\frac{\partial p}{\partial r} \approx \frac{\frac{2\sigma}{R_{eq}}}{a}\frac{h^2}{12\mu}, \qquad [35]$$

while the interface velocity predicted by the plane-film model follows from continuity

$$\pi r^2\left(-\frac{\partial h}{\partial t}\right) = 2\pi r h u; \quad u = \frac{r}{2h}\left(-\frac{\partial h}{\partial t}\right) \approx \frac{a}{2h}\left(-\frac{\partial h}{\partial t}\right). \qquad [36]$$

Combining [35] and [36] and making use of [24],

$$\frac{u_p}{u} \approx \frac{1}{4\sqrt{3k}} \frac{\mu_d}{\mu} \frac{h}{a}; \qquad [37]$$

and the approximation of plug flow is seen to be valid in the last stages of drainage, provided

$$\frac{\mu_d}{\mu} \ll 4\sqrt{3k} \frac{a}{h_c}. \qquad [38]$$

Combination of [38] and [34], making use of the expression, [29], for h_c, now yields

$$\frac{\mu_d}{\mu} \ll (12k)^{3/4} \left(\frac{8\pi\sigma R^2}{A}\right)^{1/6}. \qquad [39]$$

The right member of [39] is relatively insensitive to the values of the various physical parameters. Values of R of practical interest range from about 1 mm to 10 μm. Taking $R = 100\,\mu$m, $\sigma = 2.5 \cdot 10^{-2}$ N/m and $A = 10^{-20}$ J, [35] yields $\mu_d/\mu \ll 4 \cdot 10^2$, suggesting that the approximation of plug flow is reasonably good up to μ_d/μ-values of order 10^2.

5.3. The Neglect of Viscous Normal Stresses and of the Associated Pressure Variation

The force balance [4] on an element of film neglects the viscous (deviatoric) contribution, τ_{rr}, to the normal stress in the r-direction, while [9] neglects the corresponding contributions τ_{zz} and $(\tau_{zz})_d$ to the normal stress at the interface, together with any pressure variation, Δp_d, associated with the drop flow.

The magnitudes of these deviatoric stresses follow from [36] together with continuity:

$$\tau_{rr} = 2\mu \frac{\partial u_r}{\partial r} = \frac{\mu}{h}\left(-\frac{\partial h}{\partial t}\right). \qquad [40]$$

$$\tau_{zz} = 2\mu \frac{\partial u_z}{\partial z} = -2\frac{\mu}{r}\left(\frac{\partial (r u_r)}{\partial r}\right) = 2\frac{\mu}{h}\left(\frac{\partial h}{\partial t}\right) = -2\tau_{rr} \qquad [41]$$

and

$$(\tau_{zz})_d = 2\frac{\mu_d}{h}\left(\frac{\partial h}{\partial t}\right). \qquad [42]$$

Furthermore, the equation of creeping flow, [6], implies that

$$\Delta p_d \sim (\tau_{zz})_d. \qquad [43]$$

The neglect of the stresses is justified, provided these are small compared with the pressure difference, $2\sigma/R_{eq}$, driving the flow. Since τ_{rr} and τ_{zz} are of the same order, as are $(\tau_{zz})_d$ and Δp_d, only τ_{zz} and $(\tau_{zz})_d$ need be considered. The two requirements thus become

$$\frac{(\tau_{zz})_d}{\frac{2\sigma}{R_{eq}}} \ll 1, \quad \frac{\tau_{zz}}{\frac{2\sigma}{R_{eq}}} \ll 1. \qquad [44,45]$$

Making use of [24], [44] and [45] become

$$\frac{h_c}{a} \ll \frac{\sqrt{3}}{4}k, \quad \frac{h_c}{a} \ll \left(\frac{\sqrt{3}}{4}k\right)\frac{\mu_d}{\mu}. \qquad [46,47]$$

For the limiting condition represented by [34], [46] and [47] yield

$$\left(\frac{\mu_d}{\mu}\right)^{1/3} \ll \left(\frac{3}{4}k\right)\left(\frac{8\pi\sigma R^2}{A}\right)^{2/9} \qquad [48]$$

and

$$\left(\frac{\mu_d}{\mu}\right)^{2/3} \gg \left(\frac{4}{3k}\right)\left(\frac{A}{8\pi\sigma R^2}\right)^{2/9} \qquad [49]$$

Like the condition [39], for applicability of the plug flow approximation, [48] places an upper limit on μ_d/μ but, since $8\pi\sigma R^2/A \gg 1$, this limit is less severe and [48] is always satisfied if [39] is.

Expression [49] places a lower limit on μ_d/μ, which relates to the transition to fully-mobile drainage, resisted only by the viscosity of the continuous phase. Taking the previous values of σ, A and R, [49] requires that $\mu_d/\mu \gg 5 \cdot 10^{-3}$, suggesting that the neglect of viscous normal stresses should be a good approximation down to μ_d/μ-values of order 10^{-2}.

5.4. The Small-slope Approximation

The largest relevant interface slope arises outside the film, where the undeformed-drop equation [14*] yields

$$\mathrm{Ca}^{-1/3}\frac{\partial h}{\partial r} = \frac{\partial h^*}{\partial r^*} \sim a^* \sim 1. \qquad [50]$$

Restriction [2] is thus satisfied, provided

$$\mathrm{Ca}^{1/3} \ll 1, \qquad [51]$$

which quantifies the notion of a "gentle" collision.

If [14] rather than [14*] is taken as the starting point for the above reasoning, an alternative expression of the small-slope requirements is seen to be

$$\frac{a}{R_{eq}} \ll 1. \qquad [52]$$

Now the restriction, [49], on μ_d/μ implies, via [34], a restriction on a/R_{eq}:

$$\left(\frac{a}{R_{eq}}\right)^2 \ll \frac{9k}{4}. \qquad [53]$$

Since the right member of [53] is of order unity, [52] is seen to be roughly satisfied if [49] is.

5.5. The Neglect of Inertial Forces in the Film and in the Adjacent Drop Flow

The neglected inertial terms of the Navier–Stokes equation in the film, $\rho\,\partial u/\partial t$ and $\rho u\,\partial u/\partial r$, which can both be shown to be of order $\rho u^2/a$, may be compared with the term—$\partial p/\partial r$, which is of order $\sigma/R_{eq}a$ (ρ is the density):

$$\varepsilon = \frac{\rho u^2 R_{eq}}{\sigma} \sim \frac{\rho\sigma}{\mu_d^2}\left(\frac{A}{8\pi\sigma}\right)^{2/3} R_{eq}^{-1/3}, \qquad [54]$$

where use has been made of [24], [36] and [29]. The largest value of ε arises for small drops with low viscosities. Taking $R_{eq} = 10\,\mu m$, $\mu_d = 10^{-3}$ kg/ms, $\rho = 10^3$ kg/m^3 and the values of A and σ used previously, ε proves to be only about 10^{-4}, so the neglect of inertial forces is clearly justified.

The neglect of inertial forces in the drop flow adjacent to the film is equivalent to the assumption that this is a quasi-steady creeping flow rather than an unsteady boundary-layer flow. This, in turn, is justified provided the time scale, t_{drop}, required for such a creeping flow to adapt to changes in the film flow is much smaller than the time scale, t_{film}, of such changes:

$$\frac{t_{drop}}{t_{film}} \ll 1. \qquad [55]$$

t_{drop} is given by the time required for the vorticity to diffuse a distance of order a (the length scale of the drop flow—see paper I):

$$t_{drop} \sim \frac{a^2}{\nu_d}, \qquad [56]$$

where $\nu_d = \mu_d/\rho_d$. t_{film} is given by

$$t_{film} = \frac{h}{\dfrac{-dh}{dt}}. \qquad [57]$$

Making use of [24], [55]–[57] lead to the requirement

$$h_c \ll \frac{\frac{v_d \mu_d}{4\sigma}}{\frac{a}{R_{eq}}}. \qquad [58]$$

Like [54], [58] is independent of the flow concerned. The numerator of the right member of [58] is a length scale, of order 100 Å for low viscosity liquids such as water. Since h_c is also of this order of magnitude, [52] guarantees that [58] is satisfied. It is, however, noteworthy that for large, very low viscosity drops coalescing at free interfaces, for which a/R_{eq} is of order unity and h_c relatively large, the $\ll$ sign in [58] is replaced by a $\gg$ sign. The shear exerted by the drop phase on the interface will then be determined by an unsteady boundary layer in the drop: a situation analysed by Reed *et al.* (1974a,b) and by Ivanov & Traykov (1976).

5.6. The Neglect of Gravity and Continuous-phase Acceleration

The influence of gravity on film drainage should be negligible, provided the maximum gravitational effect on the pressure difference across the interface, of order $\Delta\rho g_0 a$, is much less than the pressure difference due to the interfacial tension, of order σ/R_{eq} ($\Delta\rho$ is the density difference, g_0 is the acceleration due to gravity):

$$\beta\left(\frac{a}{R_{eq}}\right) \ll 1, \quad \text{where } \beta = \frac{\Delta\rho g_0 R_{eq}^2}{\sigma}. \qquad [59]$$

In view of [52], [59] is satisfied, provided β is less than or of order unity. For $\Delta\rho = 10^2\ \text{kg/m}^3$ and $\sigma = 2.5 \cdot 10^{-2}\ \text{N/m}$, this will be the case, provided $R_{eq} \leqslant 5\ \text{mm}$—a condition which is satisfied in virtually all cases.

A reference frame translating with colliding drops will, in general, be an accelerated one and this acceleration, **g**, enters into the equations describing the drainage process as an additional effective contribution, $-\mathbf{g}$, to the acceleration due to gravity. Typically

$$|\mathbf{g}| \sim \frac{U^2}{L}, \qquad [60]$$

where U and L denote the system velocity and length scales. For large stirred vessels U^2/L is typically less than or of the order of g_0. In small high-velocity flows, U^2/L may be 2 or more orders of magnitude larger than g_0 and the maximum permissible value of R_{eq} is, accordingly, an order of magnitude or more smaller. In such flows, however, drop break-up will, in general, ensure that actual R_{eq}-values are much smaller still, so that neglect of any influence of g on drainage is amply justified.

6. CONCLUDING REMARKS

The process of film drainage during drop collisions in liquid–liquid dispersions is determined by boundary conditions provided by the external flow, consisting of a time-dependent interaction force or approach velocity. The present results indicate the very substantial influence of these boundary conditions on the drainage process: drainage rates following drop flattening decrease much less rapidly in the constant-velocity case than in the constant-force case and differ by as much as an order of magnitude in the final stages of drainage. This emphasizes the importance of simulating the actual time-dependent boundary conditions in the modelling of coalescence in liquid–liquid dispersions.

The effect of the van der Waals forces is to accelerate drainage in the thinnest zone of the film, rapidly leading to rupture once these forces become comparable in magnitude with the capillary forces responsible for the earlier stages of drainage. For cases in which flattening precedes the onset of van der Waals effects, the effective critical film-rupture thickness, h_c, is well-predicted by the simple expression proposed in paper I ([28], taking an optimized coefficient [29]). The drainage time, t_c, is then given with sufficient precision for practical purposes by the use of h_c in the asymptotic drainage expression [20].

Acknowledgement—The authors gratefully acknowledge the financial support of ICI for this work.

REFERENCES

CHESTERS, A. K. 1988 Drainage of partially mobile films between colliding drops: a first-order model. In *Proc. Euromech*, Toulouse, France, p. 234.

CHESTERS, A. K. 1991 The modelling of coalescence processes in fluid-liquid dispersions: a review of current understanding. *Trans. Instn Chem. Engrs* **69,** 259–270.

CHESTERS, A. K. & HOFMAN, G. 1982 Bubble coalescence in pure liquids. *Appl. Scient. Res.* **38,** 353–361.

DAVIS, R. H., SCHONBERG, J. A. & RALLISON, J. M. 1989 The lubrication force between two viscous drops. *Phys. Fluids A* **1,** 77–81.

HIEMENZ, P. C. 1986 *Principles of Colloid and Surface Chemistry*, 2nd edn. Dekker, New York.

IVANOV, I. B. & TRAYKOV, T. T. 1976 Hydrodynamics of thin liquid films rate of thinning of emulsion films from pure liquids. *Int. J. Multiphase Flow* **2,** 397–410.

REED, X. B., RIOLO, E. & HARTLAND, S. 1974a The effect of hydrodynamic coupling on the axisymmetric drainage of thin films. *Int. J. Multiphase Flow* **1,** 411–436.

REED, X. B., RIOLO, E. & HARTLAND, S. 1974b The effect of hydrodynamic coupling on the thinning of a film between a drop and its homophase. *Int. J. Multiphase Flow* **1,** 437–464.

YIANTSIOS, S. G. & DAVIS, R. H. 1990 On the buoyancy-driven motion of a drop towards a rigid surface or a deformable interface. *J. Fluid Mech.* **217,** 547–573.

YIANTSIOS, S. G. & DAVIS, R. H. 1991 Close approach and deformation of two viscous drops due to gravity and van der Waals forces. *J. Colloid Interface Sci.* **144,** 412–433.

APPENDIX

Surface Increase and Related Interaction Force of Flattened Drops

Surface increase

Figure 5 depicts a simplification of the geometry of equal flattened drops. The thickness of the film has been neglected and the transition from the plane film to the spherical external interface approximated as abrupt. Note that this implies an infinite interface curvature at the film edge. In the more general case of unequal drops, the film is spherical with a radius of curvature, R_c, given by [11c].

Since both drops are indented, volume conservation requires that the radius of the spherical portion increases: $R \to R'$. In the limit of small deformations, [52], the volume of the missing (indented) portion of this larger sphere is found from elementary geometrical considerations to be the same for both drops, given by $\pi r_f^2/4R_{eq}$, where r_f denotes the film radius. The value of R' then follows from volume conservation:

$$\frac{R'}{R} = 1 + \frac{r_f^4}{16R^3R_{eq}}. \qquad [A1]$$

The surface area of a drop now follows from the sum of its spherical portions and its increase, ΔS, proves to be the same for both drops, given by

$$\Delta S = \frac{\pi r_f^4}{4R_{eq}^2}. \qquad [A2]$$

The value of r_f is related to the indentation distance Z (the sum of the drop radii minus the separation of their centres):

$$Z = \frac{r_f^2}{R_{eq}}; \qquad [A3]$$

and [A2] can, therefore, be written as

$$\Delta S = \frac{\pi Z^2}{4}. \qquad [A4]$$

Interaction force

The drop interaction force, F, is readily obtained from energy considerations:

$$FdZ = \sigma d(2\Delta S); \qquad [A5]$$

the left member representing the work done in increasing Z and the right member the resulting increase in the free energy of the system. Combination of [A4] and [A5] yields

$$F = \pi\sigma Z. \qquad [A6]$$

It is noteworthy that, with the help of [A3], F can be expressed as

$$F = \pi r_f^2\left(\frac{\sigma}{R_{eq}}\right). \qquad [A7]$$

which is half the value obtained by multiplying the pressure in the film, $2\sigma/R_{eq}$, by the film area. Evidently the contribution to F of the pressure singularity associated with the infinite curvature at the film edge is significant.

Making use of [17], [A6] becomes

$$a^2 = \frac{R_{eq}Z}{2} = \frac{R_{eq}}{2}(Vt - h_0), \qquad [A8]$$

which transforms to [18].